BUTTERWORTH HEINEMANN

Molecular modeling studies of the artemisinin (qinghaosu)–hemin interaction: Docking between the antimalarial agent and its putative receptor

Kanhiya L. Shukla,* Tamara M. Gund,* and Steven R. Meshnick,†

**Department of Chemistry and Chemical Engineering, New Jersey Institute of Technology, Newark, NJ, USA*
†Department of Epidemiology, University of Michigan School of Public Health, Ann Arbor, MI, USA

Artemisinin (qinghaosu, QHS) is a promising new antimalarial agent that is effective against drug-resistant strains of malaria. The antimalarial activity of this drug appears to be mediated by an interaction of the drug's endoperoxide bridge with intraparasitic hemin. We have carried out a computer-assisted docking of QHS with hemin from various starting configurations and found that, in the most stable docked configuration, the endoperoxide bridge is in close proximity to the hemin iron. In contrast, an inactive analog, deoxyartemisinin (DQHS), docks in a different manner. Further computer analysis of the drug–hemin interaction might aid in the design of new QHS congeners.

Keywords: artemisinin, docking, qinghaosu, hemin, malaria, antimalarial, molecular modeling

INTRODUCTION

Malaria is a major health problem in lesser developed countries, affecting an estimated 270 million people per year and killing 1–2 million per year.[1] Drug-resistant strains of the malaria parasite, particularly *Plasmodium falciparum*, have become widespread.[1] As a result, new antimalarial agents are needed.

Artemisinin (qinghaosu [QHS]; Figure 1) and its derivatives are promising new antimalarial agents that are effective against strains of malaria resistant to the older drugs.[2,3] QHS was isolated from a 2000-year-old Chinese herbal remedy. QHS derivatives have been widely used in China, where over 2 million doses of one derivative, artemether, have been given.[1] QHS derivatives are faster acting than quinine and are particularly effective against cerebral malaria. No adverse drug effects have ever been reported.

The antimalarial action of QHS appears to be mediated by the generation of free radicals from the endoperoxy bridge of the drug. This bridge is essential for antimalarial activity because derivatives having one oxygen instead of two are inactive (i.e., desoxyartemisinin [DQHS]; Figure 1).[4,5] The role of free radicals in the mechanism of action of QHS is implied by the fact that free radical scavengers antagonize the antimalarial effect of this drug,[6–8] and that lipid peroxidation end products can be detected in QHS-treated parasites.[7]

Intraparasitic hemin plays a critical role in the mechanism of action of QHS.[9] In the process of degrading hemoglobin, malaria parasites accumulate hemin as an insoluble polymer known as hemozoin.[10–13] Strains of *Plasmodium berghei* lacking hemozoin are insensitive to QHS.[14] Hemin (Figure 1) has previously been proposed as the receptor for other antimalarial drugs such as chloroquine,[15] quinine,[16] and mefloquine.[15] Thus, the presence of hemin in malaria parasites may be the explanation for their sensitivities to several antimalarial drugs.

Hemin reacts with QHS in several ways. First, hemin catalyzes the decomposition of QHS. This was shown by cyclic voltammetry, in which the reduction potential of

Color plates for this article are on pages 235 and 236.

Address reprint requests to Dr. Gund, Department of Chemistry and Chemical Engineering, New Jersey Institute of Technology, University Heights, Newark, NJ 07102, USA.
Received 23 June 1992; revised 10 October 1993, 8 July 1994; accepted 25 August 1994.

655 Avenue of the Americas, New York, NY 10010

0263-7855/95/$10.00
SSDI 0263-7855(94)00001-9

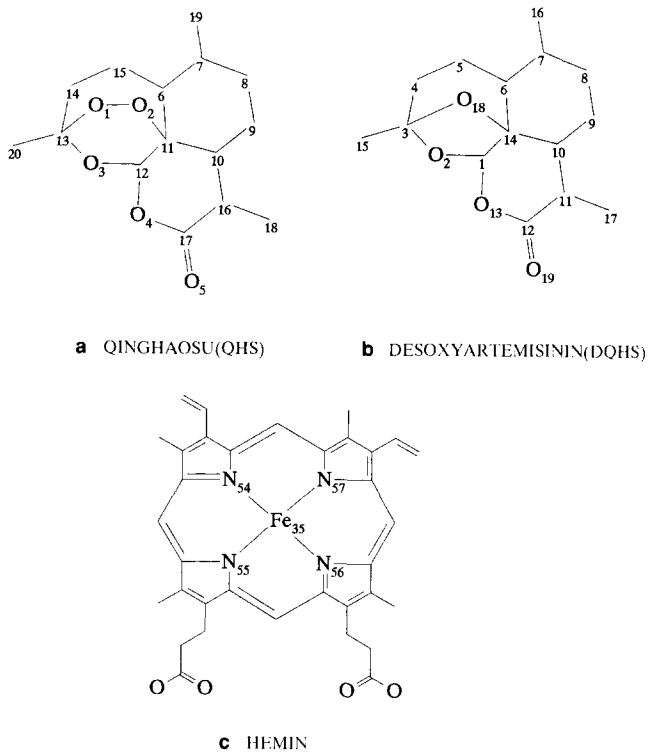

Figure 1. Structures and relevant numbering system of the molecules investigated. (a) Artemisinin (qinghaosu, QHS); (b) desoxyqinghaosu (DQHS); (c) hemin.

QHS changed from −1.0 to −0.45 V in the presence of catalytic amounts of hemin.[17] Second, QHS alkylates hemin to form a covalent adduct.[10–13] This reaction occurs in vivo because the adduct appears to form in [^{14}C]QHS-treated *P. falciparum*-infected erythrocytes.[9] Third, the reaction between QHS and hemin liberates oxidants that cause the loss of thiols from erythrocyte membranes in vitro.[9]

In this article we use molecular modeling techniques to find the most energetically favorable modes of binding between the antimalarial QHS and hemin as well as between the inactive analog, DQHS, and hemin.

METHODS

The modeling work was performed using an Evans and Sutherland PS330 computer graphics system coupled to a VAX 6430, and the IRIS Silicon Graphics D20 workstation. The software used included CHEMX (version October 1991),[18] and SYBYL (version 6.0).[19] Docking was performed using the SYBYL software set on default parameters. The details of the docking procedure are described below. Electrostatic isopotential curves were derived using the SYBYL Gasteiger charges.

The X-ray structures of hemin, DQHS, and artemether (the methoxy derivative of QHS) were obtained from the Cambridge Crystallographic Data Bank.[20] Hemin was modeled in the iron(III) and iron(II) oxidation states. QHS was built from the X-ray structure of artemether. Figure 1 shows the structures and the numbering scheme of the atoms for the molecules investigated.

RESULTS

Structures of QHS, DQHS, and hemin

Both QHS and DQHS have similar structures with polar and nonpolar regions (Figure 1). The polar regions, where the oxygens are clustered, are negatively charged. Color Plate 2a and b shows the isopotential curves of QHS and DQHS at −20 kcal/mol. For QHS the isopotential curves are distributed into two main regions, one covering the endoperoxide oxygens (O_1 and O_2) and the other the three remaining oxygens. For DQHS the isopotential curves at −20 kcal/mol are distributed mainly toward the three nonendoperoxide oxygens and a small region toward the endoperoxide O_{18} oxygen. Hemin is a planar molecule with a strong positive charge on its central iron atom, which lies slightly above the plane of the molecule. The structure of hemin was taken from the Cambridge Crystallographic Data Bank. Charges on the iron were assigned as +2 and +1 but the structures were kept the same. Gasteiger charges for the molecules with the two iron states were calculated, and from the Gasteiger charges isopotential curves were derived at +50 kcal/mol. These are shown in Figure 2c. The two sides of the porphyrin ring are unequally distributed, with a stronger and larger positive region being on the side with the iron pointing up. Hemin (Fe^{2+}) has a larger +50 isopotential area (purple) than hemin (Fe^{+}, yellow). The two states of iron were considered because these would correspond to the two oxidation states of iron [iron(III) and iron(II)]. Because SYBYL and other modeling packages are not completely parameterized for iron, the charges had to be assigned by an approximation. We looked at several model metals and calculated the change in charge distribution on the metal after allowing dispersion of the charge throughout the molecule. Thus for hemin in which the iron is substituted by aluminum, an assignment of a +3 charge on aluminum results in an actual charge of about +2 on aluminum after dispersal of charge on the whole molecule. Therefore the two iron oxidation states of iron(III) and iron(II) were assigned actual charges of +2 and +1. The actual charge is not as important as the changes that are observed with difference in charge. Both cases gave similar results, as is explained below.

Computer-assisted molecular modeling

QHS has two prominent negative regions and both may interact with the porphyrin iron bridge. Because DQHS is inactive it was presumed that the main interaction in QHS was between the peroxide oxygen bridge and the hemin iron. Docking was performed to test whether the peroxide bridge performs an important role in binding to hemin.

Dockings were performed from several different starting configurations. For hemin, the least-squares plane of the porphyrin ring was determined and oriented in the *xy* plane. The iron may point up (+) or down (−) in the *z* direction (Figure 1c); both orientations were examined. Two oxidation states of hemin [iron(III) and iron(II)] were also examined. In the initial starting configurations there were no differences, and therefore only the initial interacting orientations of hemin [iron(III)] are shown (Figures 3 and 4).

QHS and DQHS were oriented in different ways to test

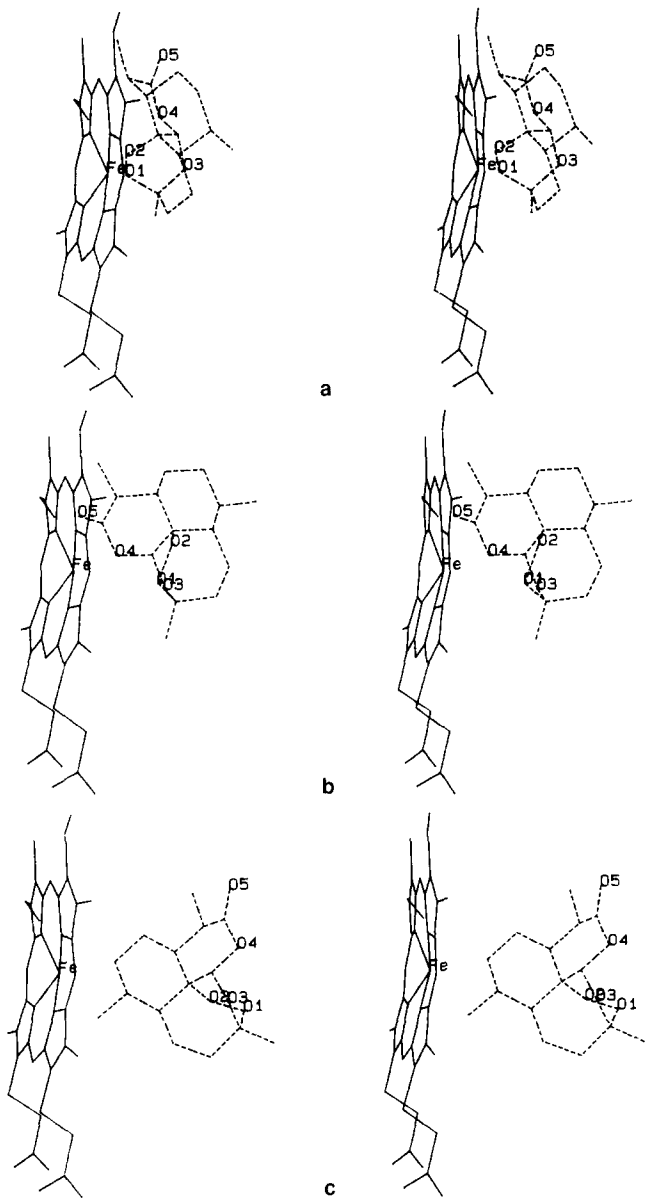

Figure 2. Undocked configurations of hemin and QHS. The planes of the atoms are perpendicular to the plane of the paper. (a) Initial configuration QHI-1: hemin and QHS (QI-1); (b) initial configuration QHI-2: hemin and QHS (QI-2); (c) initial configuration QHI-3: hemin and QHS (QI-3).

the most favorable modes of interaction between the oxygens of the drug molecules and hemin. Planes were drawn through the molecules and lined up parallel to the plane of the porphyrin ring. Distances were measured from the centers of these planes to the center of the porphyrin ring plane.

For QHS three orientations for docking with hemin were used. In each case the following set of atoms was placed in the *xy* plane (represented by the plane of the paper): (1) the seven-membered ring atoms O_3, C_{12}, C_{11}, C_6, C_{15}, C_{14}, and C_{13} (QI-1); this orientation aligned the peroxide isopotentials with the larger fraction of the hemin iron isopotential. The interacting atoms were O_1 and O_2 of QHS with the iron pointing up; (2) the ring atoms O_3, C_{12}, C_{11}, O_2, O_1, and C_{13} (QI-2); this orientation placed the larger isopotential area toward the larger iron isopotential area. The interacting atoms were O_5, O_4, and O_3 of QHS, with hemin iron pointing up; (3) the atoms O_1, O_2, O_3, O_4, and O_5 (QI-3); here the maximum number of oxygens (O_1–O_5) was being tested for interaction with iron. The three modes of interaction can be seen in Figure 1a and are shown in Figure 3a–c.

For DQHS two orientations with the following atoms in the *xy* plane were used: (1) the seven-membered ring atoms O_2, C_1, C_{14}, C_6, C_5, C_4, and C_3 (DQI-1); this orientation places the large nonperoxide potential of DQHS with the large iron potential. The interacting oxygen atoms of DQHS were O_2 and O_{13} with the larger isopotential of iron; (2) the five-membered ring atoms O_2, C_1, C_{14}, O_{18}, and C_3 (DQI-2); this places the potential due to O_{19} and O_{13} in an orientation to interact with the large iron potential. These interactions can be seen in Figure 1b and are shown in Figure 4a and b.

QHS and DQHS were placed at initial distances of ±3, ±4, ±5, ±6, and ±7 Å from hemin and docked using the SYBYL protocol. During the docking process energetically favorable orientations were allowed to take place and final interaction energies were calculated. Many forces are involved in the intermolecular association: hydrophobic, dispersion or van der Waals, hydrogen bonding, and electrostatic (ion pairing). The major driving force for binding appears to be hydrophobic interactions, but the specificity of the binding appears to be controlled by hydrogen bonding and electrostatic interactions.[21–23] Figure 3 shows the initial interactive configuration of hemin and QHS for the three initial orientations of QHS that produced the lowest energy

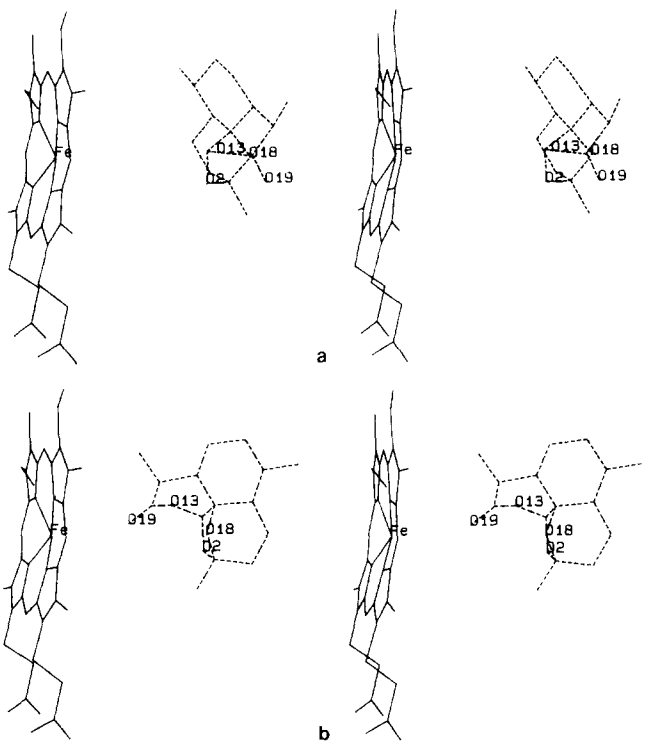

Figure 3. Undocked configurations of hemin and DQHS. (a) Initial configuration DQHI-1: hemin and DQHS (DQI-1); (b) initial configuration DQHI-2: hemin and DQHS (DQI-2).

final configurations. Figure 4 shows the initial interactive configurations of DQHS and hemin that produced the lowest energy final configurations for this set. Figures 5 and 6 show the minimum energy configurations of QHS and DQHS after docking to hemin [iron(III)]. Figures 7 and 8 show the minimum energy configurations after docking to hemin [iron(II)].

QHS orientation (QI-1) on docking to hemin [iron(III)] produced the minimum energy configuration QHF-1 shown

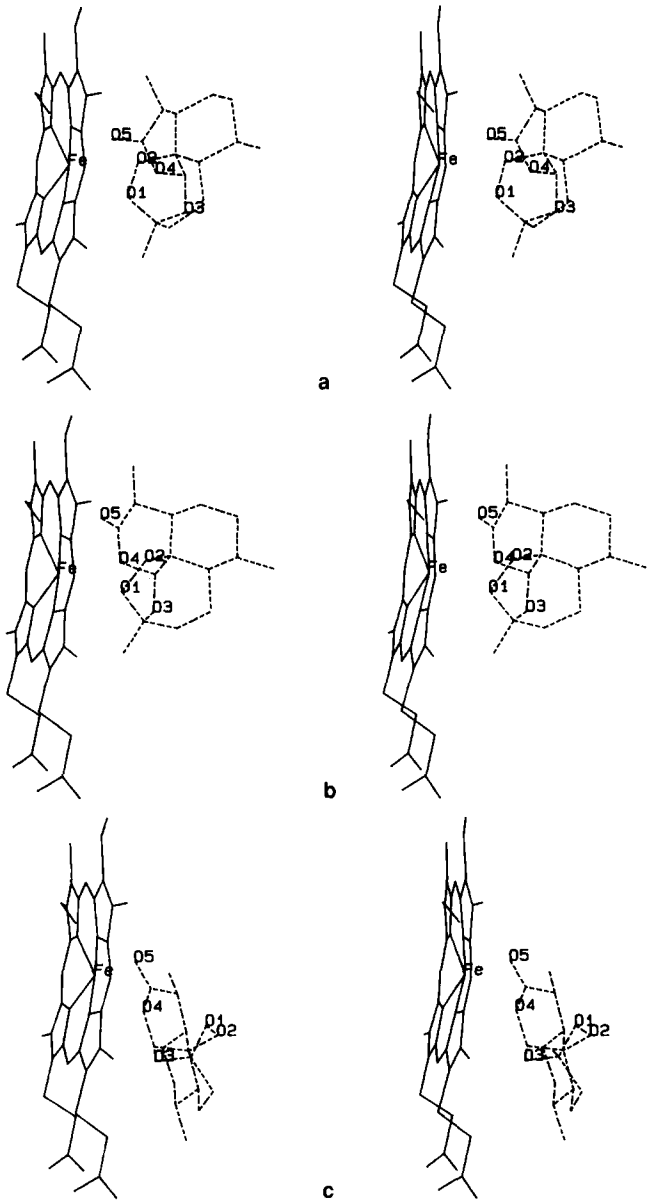

Figure 4. Docked configurations of hemin [iron(III)] and QHS. (a) Final configuration QHF-1: minimum energy, 220 kcal/mol; peroxide bridge oxygens (O_1 and O_2) and oxygen O_5 interact preferentially with the hemin iron. (b) Final configuration QHF-2: minimum energy, 224.5 kcal/mol; peroxide bridge oxygen O_1 and nonperoxide oxygen O_4 preferentially interact with the hemin iron. (c) Final configuration QHF-3: minimum energy, 221.6 kcal/mol; nonperoxide bridge oxygens O_3, O_4, and O_5 interact preferentially with the hemin iron.

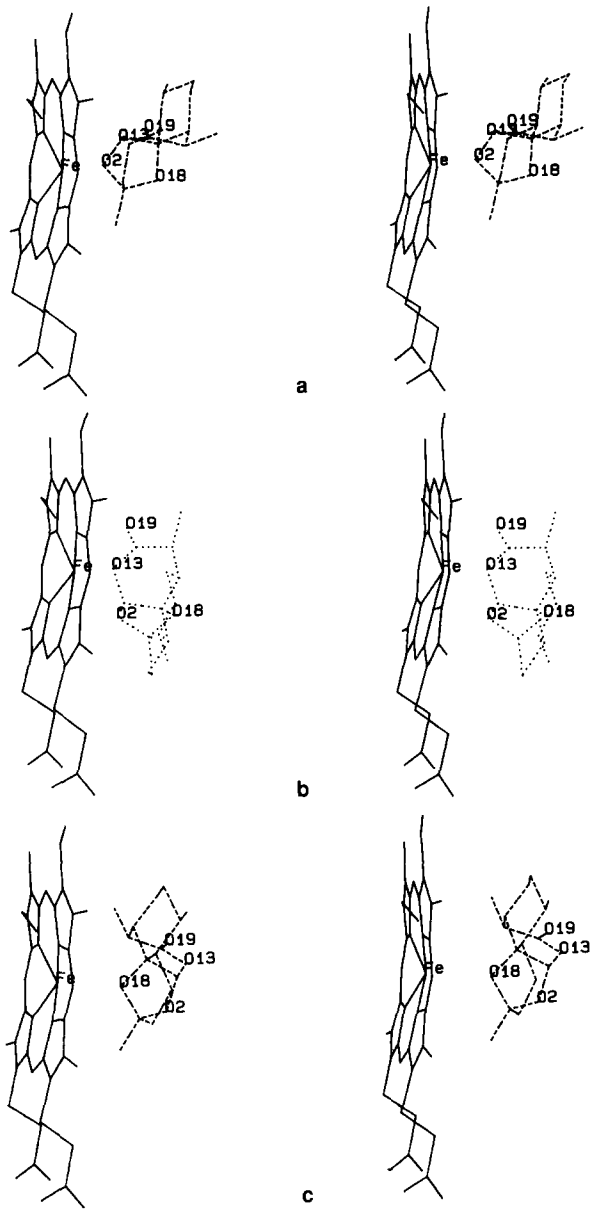

Figure 5. Docked configurations of hemin [iron(III)] and DQHS. (a) Final configuration DQHF-1: minimum energy, 211.9 kcal/mol; nonperoxide bridge-derived oxygens O_2 and O_{13} interact preferentially with the hemin iron. (b) Final configuration DQHF-2: minimum energy, 209.4 kcal/mol; nonperoxide bridge-derived oxygens O_2, O_{13}, and O_{19} interact preferentially with the hemin iron. (c) Final configuration DQHF-3: minimum energy, 225.4 kcal/mol; peroxy-derived oxygen O_{18} interacts preferentially with the hemin iron.

in Figure 5a. Here three oxygens (including the two from the peroxide bridge) are in closer proximity to the positive iron than the other two. The respective distances of the oxygens with respect to the iron are given in Table 1. Orientation (QI-2) on docking produced the configuration QHF-2 (Figure 5b), 4.5 kcal higher in energy than QHF-1. In this configuration two oxygens bind to the iron: the peroxide bridge oxygen (O_1) and the nonperoxide oxygen O_4. Table 1A gives the O–Fe distances. Orientation QI-3 pro-

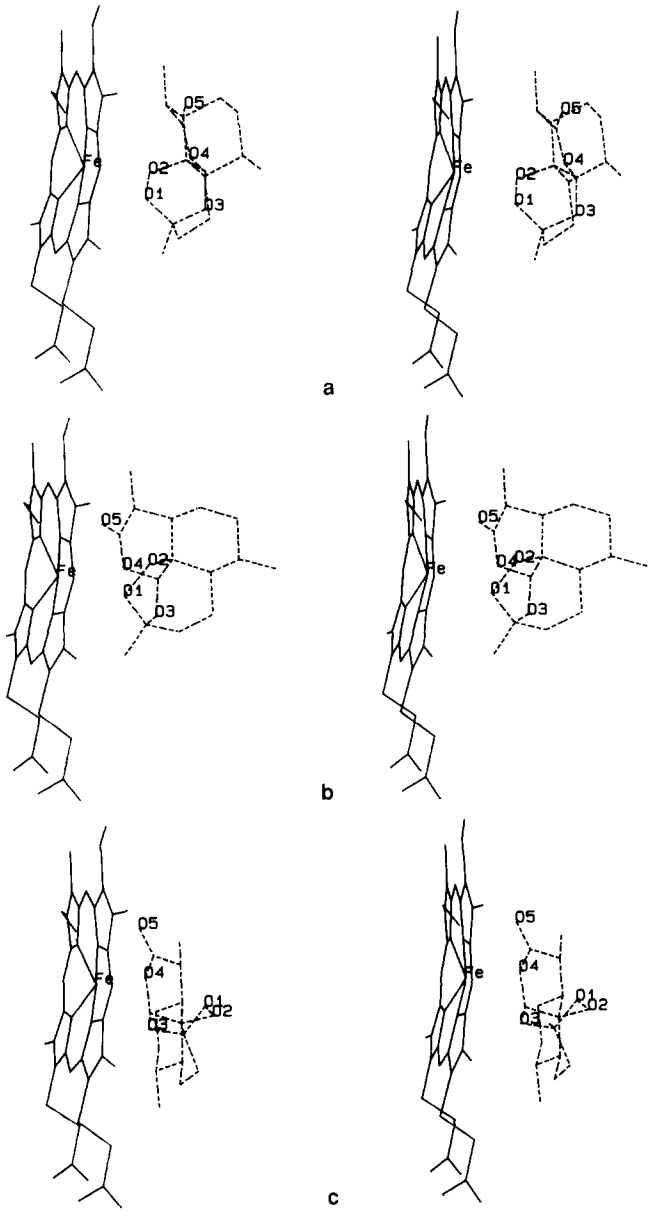

Figure 6. Docked configurations of hemin [iron(II)] and QHS. (a) Final configuration QHF-4: minimum energy, 233.3 kcal/mol; peroxide bridge oxygens (O_1 and O_2) interact preferentially with the hemin iron. (b) Final configuration QHF-5: minimum energy, 233.7 kcal/mol; peroxide bridge oxygen O_1 and nonperoxide oxygen O_4 preferentially interact with hemin iron. (c) Final configuration QHF-6: minimum energy, 233.5 kcal/mol; peroxide bridge oxygen O_1 and nonperoxide oxygen O_4 interact preferentially with the hemin iron.

duced a minimum energy docked configuration of hemin [iron(III)] and QHS (QHF-3) (Figure 5c) that was 1.6 kcal/mol higher in energy than QHF-1. In this configuration binding is strongest with the nonperoxide oxygens (O_3, O_4, and O_5) (Table 1). Oxygens O_4 and O_5 were actually at a closer distance than O_3 (2.54, 2.61, and 3.92 Å, respectively). When the same procedure was performed for DQHS the two starting orientations (DQI-1 and DQI-2) produced final docked configurations DQHF-1 and DQHF-2 (Figure 6a and b) that differed by 2.5 kcal/mol. In both cases, the single oxygen homolog (O_{18}) of the endoperoxide bridge was not near the iron. The distances between the oxygens and iron for the two configurations are given in Table 1B. In each case the oxygen homologous to the peroxide bridge was at a greater distance from the hemin iron (4.29 and 4.32 Å) than the other three oxygens. Docking procedures were performed to test docked orientations in which this latter oxygen (O_{18}) interacted with the hemin iron (Figure 6c).

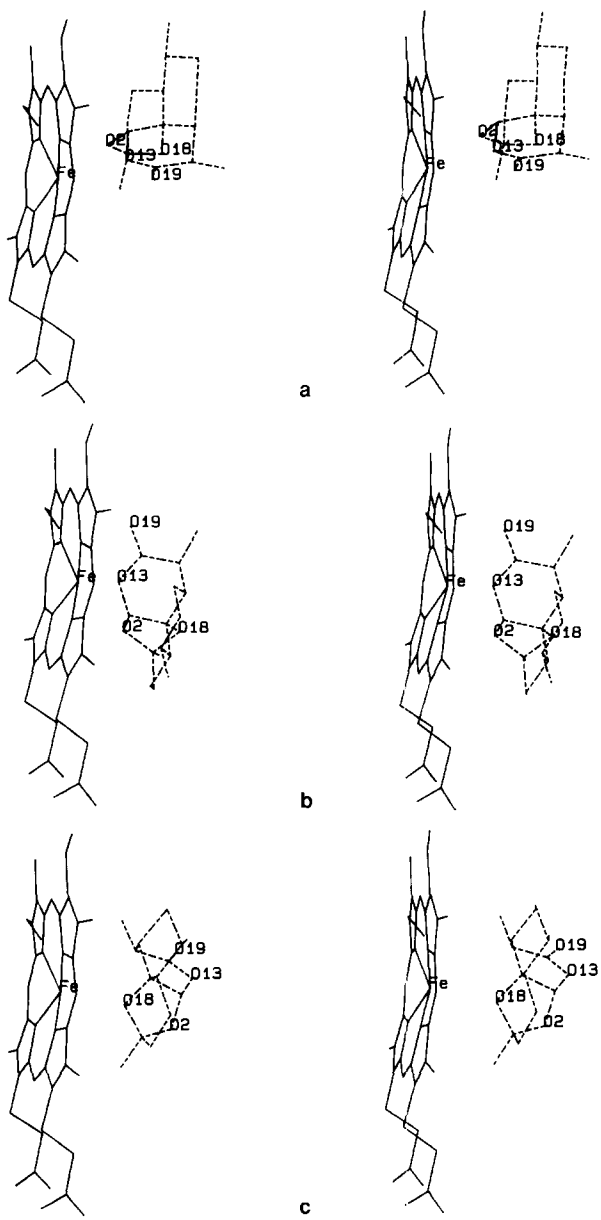

Figure 7. Docked configurations of hemin [iron(II)] and DQHS. (a) Final configuration DQHF-4: minimum energy, 225.3 kcal/mol; nonperoxide bridge-derived oxygens O_2 and O_{13} interact preferentially with the hemin iron. (b) Final configuration DQHF-5: minimum energy, 223.6 kcal/mol; nonperoxide bridge-derived oxygens O_2, O_{13}, and O_{19} interact preferentially with the hemin iron. (c) Final configuration DQHF-6: minimum energy, 228.0 kcal/mol; peroxy-derived oxygen O_{18} interacts preferentially with the hemin iron.

Table 1. Energy and oxygen distances of docked configurations

Docked configuration	Energy (kcal/mol)	Difference in energy from QHF-1 (kcal/mol)	Fe–O distance				
			O_1	O_2	O_3	O_4	O_5
A. QHS–hemin [iron(III)] configurations							
QHF-1	220.0	0.0	2.56	2.82	4.78	3.67	2.70
QHF-2	224.5	4.5	2.57	3.47	4.04	2.88	3.80
QHF-3	221.6	1.6	4.60	5.41	3.92	2.54	2.61

B. DQHS–hemin [iron (III)] configurations						
		Difference in energy from DQHF-2 (kcal/mol)	Fe–O distance			
			O_2	O_{13}	O_{18}	O_{19}
DQHF-1	211.9	2.5	2.50	2.50	4.29	3.92
DQHF-2	209.4	0.0	2.59	2.56	4.32	2.63
DQH-3	225.4	16.0	4.60	5.74	2.51	6.53

C. QHS–hemin [iron (II)] configurations							
		Difference in energy from QHF-4 (kcal/mol)	Fe–O distance				
			O_1	O_2	O_3	O_4	O_5
QHF-4	233.3	0.0	2.63	2.65	4.92	4.40	5.23
QHF-5	233.7	0.4	2.70	3.60	4.22	3.10	3.86
QHF-6	233.5	0.2	2.81	3.84	4.17	3.05	3.74

D. DQHS–hemin [iron (II)] configurations						
		Difference in energy from DQHF-5 (kcal/mol)	Fe–O distance			
			O_2	O_{13}	O_{18}	O_{19}
DQHF-4	225.3	1.7	2.63	2.71	4.53	4.27
DQHF-5	223.6	0.0	2.71	2.67	4.50	3.39
DQHF-6	228.0	4.4	4.82	5.82	2.67	6.63

The energy of this configuration was higher by 16 kcal/mol than the lowest energy configuration DQHF-1.

The docking procedures just described were also performed with hemin [iron(II)]. In this case the QHS–hemin orientations QHI-1, QHI-2, and QHI-3 produced the final orientations QHF-4, QHF-5, and QHF-6 shown in Figure 7. Although the binding mode varied, the energies of the three configurations were almost identical (0.2 kcal/mol). Configuration QHF-4 had the peroxide oxygens O_1 and O_2 closest to the hemin iron (2.63 and 2.65 Å) with oxygens O_3, O_4, and O_5 further removed (4.92, 4.40, and 5.23 Å). Configuration QHF-5 and QHF-6 were almost identical. In both cases O_1 (2.70 and 2.81 Å) and O_4 (3.10 and 3.05 Å) were closest, with the other three oxygens being further away: O_3 (4.22 and 4.17 Å), O_2 (3.61 and 3.84 Å), and O_5 (3.86 and 3.74 Å). Table 1C summarizes these results. For DQHS orientations DQ-1 and DQ-2 produced final orientations DQHF-4 and DQHF-5, which were 1.7 kcal/mol apart in energy. Both configurations involved interactions with the nonperoxide-derived oxygens. In configuration DQHF-4 (1.7 kcal/mol higher than DQHF-5) O_2 and O_{13} were closer (2.63 and 2.71 Å) than O_{18} and O_{19} (4.53 and 4.27 Å). Configuration DQHF-5 varied somewhat, with O_2 and O_{13} being closer (2.71 and 2.67 Å) than O_{19} and O_{18} (3.39 and 4.50 Å). These results are summarized in Table 1D. Forcing the interaction with peroxide O_{18} gave the configuration DQHF-6, shown in Figure 6c and Table 1D, that was 4.4 kcal/mol higher in energy than DQHF-4.

DISCUSSION

To better understand the mechanism of action of the antimalarial QHS, computer-aided docking procedures were performed between the drug and its putative receptor. Which final docked configurations were obtained depended partly on the electrostatic configuration of the hemin. For QHS the lowest energy docking configuration with hemin [iron(III) or iron(II)] places the endoperoxide bridge in close proximity to the hemin iron. In contrast, for the inactive analog DQHS a different portion of the molecule is in proximity to the iron.

Several different starting configurations were used for the docking between QHS and hemin. In all cases, the molecules reoriented themselves to one of two most favorable configurations. Interaction of QHS with hemin [iron(III)] involves binding between the endoperoxide (O_1 and O_2) bridge and O_5 of QHS to the front of the hemin iron bridge (Figure 5a). However, binding of QHS to hemin [iron(III)] involving the nonperoxide oxygens (O_3, O_4, and O_5) produces a docked configuration that is only 1.6 kcal/mol higher in energy than the lowest energy state (Figure 5c). The least favorable configuration (4.5 kcal/mol higher in energy than the lowest state) for binding of QHS appears to involve one peroxide oxygen (O_1) and oxygen O_4. Thus, with hemin [iron(III)] of the three modes of interaction, the binding involving the peroxide bridge oxygens and O_5 is about 4.5 kcal/mol lower in energy (Table 1), suggesting that this is the preferred mode of interaction; however, binding with the nonperoxide oxygens can be competitive (1.6 kcal/mol higher in energy). Interaction of QHS with hemin [iron(II)], however, gives configurations of almost equal energy, in which the interactions with the full peroxide bridge O_1 and O_2 are lowest in energy by only 0.2 kcal/mol. Thus in this case the interactions with both sides of QHS are even more competitive.

DQHS has a single oxygen instead of the peroxide bridge. The hemin iron could interact with DQHS in several ways. We expected that the hemin iron could preferentially interact either at the side involving the three nonperoxide oxygens O_2, O_{13}, and O_{19}, or the peroxide-derived oxygen O_{18} (Figures 1b and 2b). Two low-energy modes of binding were found for both hemin [iron(III)] and hemin [iron(II)] (Table 1). All involved nonperoxide oxygens. The configurations with the three oxygens binding O_2, O_{13}, and O_{19} (Table 1, Figures 6b and 8b) were 2.5 and 1.7 kcal/mol lower in energy than the configurations with two nonperoxide oxygens binding (O_2 and O_{13}; Table 1, Figures 6a and 8a). In fact, the configuration with the peroxide-derived oxygen O_{18} binding is 16 kcal/mol higher in energy (Table 1, Figure 6c) for hemin [iron(III)] and 4.4 kcal/mol higher for hemin [iron(II); Figure 8c].

Thus, the active antimalarial QHS clearly interacts with hemin in a manner different from its inactive analog DQHS.

In the most favorable docking configuration for hemin and QHS, the iron is between 2.6 and 2.8 Å from each of the oxygens in the endoperoxide bridge. The binding process can be explained by looking at the electrostatic interactions involved during docking. For QHS two available sides of binding are clearly seen (Figure 2a): the smaller region around the peroxide bridge and a larger region encompassing the other three oxygens. For the lowest energy docked configuration, the process began by orienting the molecules so that the peroxide oxygen would be closer to the hemin iron. The positive iron field is placed in an environment to interact with the negative (−20 kcal/mol) field of QHS (peroxide oxygens). After docking QHS reorients itself so that the negative field of three oxygens (O_1, O_2, and O_5) and peroxide interact with the positive field of the iron. The nature of the binding of QHS with hemin [iron(III) and iron(II)] can also be seen in the space-fill representation of the lowest energy docked configuration (Figure 9a and b). The bridge oxygens are easily accommodated by the porphyrin iron environment. Whether two or three oxygens are accommodated is dependent on the oxidation state of iron.

For DQHS the most stable arrangement is accommodated by interacting with the three nonperoxide oxygens. Figure 10 shows the space-fill view of the favored docked configurations. A stable arrangement appears but the peroxide bridge is not involved.

In conclusion, we have shown that the lowest energy binding mode for QHS and hemin involves the side containing the endoperoxide bridge, but that QHS appears to be able to interact from the nonperoxide bridge side as well. Variation in binding occurs, depending on the oxidation state of iron. For iron(III) the low-energy binding mode involves the two endoperoxide oxygens O_1 and O_2, and oxygen O_5. For iron(II), all three modes of binding are almost of the same energy but the lowest energy mode involves only the endoperoxide bridge oxygens O_1 and O_2. DQHS and hemin bind preferentially from the side not involving the peroxide-derived oxygens. Because this molecule is inactive it appears that the endoperoxide bridge is important for antimalarial activity.

QHS might be able to intercalate between two heme molecules that tend to "stack" in solution.[24] On the other hand, this should not occur in malarial pigment (hemozoin), in which heme molecules are polymerized so that the carboxy group of one heme is bound to the iron atom of another.[25] This is consistent with the observation that QHS appears to react predominantly with free heme molecules that have not yet been incorporated into hemozoin.[10]

Heme catalyzes the breakdown of artemisinin[17] into a free radical[11] and/or electrophilic intermediate.[12] Once formed, this intermediate can alkylate heme[10] or protein.[13] The orientation of QHS with respect to heme may be critical to formation of this intermediate and, thus, for drug action. Thus, molecular docking studies may aid in the design of new QHS congeners.

Further studies might involve preparing QHS derivatives that lack the carbonyl oxygen O_5.

ACKNOWLEDGMENTS

This work was supported by NIH Grant AI26848 and by a grant from the UNDP/World Bank/WHO Special Programme for Research and Training in Tropical Diseases.

REFERENCES

1 UNDP/World Bank/WHO Special Programme for Research and Training in Tropical Diseases. Tropical Dis-

eases. Progress in Research, 1989–1990. World Health Organization, Geneva, Switzerland, 1991, p 29
2 Klayman, D.L. *Science* 1985, **228,** 1049
3 Luo, X.D. and Shen, C.C. *Med. Res. Rev.* 1987, 29
4 China Cooperative Research Group on Qinghaosu and Its Derivatives as Antimalarials. Chemical studies on qinghaosu (artemisine). *J. Traditional Chin. Med.* 1982, **2,** 3
5 Brossi, A., Venugopaplan, B., Gerpe, L.D., Yeh, H.J.C., Flippen-Anderson, J.L., Luo, X.D., Milhous, W., and Peters, W. *J. Med. Chem.* 1988, **31,** 645
6 Krungkrai, S.R. and Yuthavong, Y. *Trans. R. Soc. Trop. Med. Hyg.* 1987, **81,** 710
7 Meshnick, S.R., et al. *Prog. Clin. Biol. Res.* 1989, **313,** 95
8 Levander, O.A., Ager, A.L., Morris, V.C., and May, R.G. *Am. J. Clin. Nutr.* 1989, **50,** 346
9 Meshnick, S.R., Thomas, A., Ranz, A., Xu, C.M., and Pan, H.Z. *Mol. Biochem. Parasitol.* 1991, **49,** 181
10 Hong, Y.L., Yang, Y.-Z., and Meshnick, S.R. *Mol. Biochem. Parasitol.* 1994 (in press)
11 Meshnick, S.R., Yang, Y.-Z., Lima, V., Kuypers, F., Kamchonwongpaisan, S., and Yuthavong, Y. *Antimicrob. Agents Chemother.* 1993, **37,** 1108
12 Posner, G. and Oh, C.H. *J. Am. Chem. Soc.* 1992, **114,** 8328
13 Yang, Y.-Z., Asawamahasakda, W., and Meshnick, S.R. *Biochem. Pharmacol.* 1993, **46,** 336
14 Peters, W., Lin, L., Robinson, B.L., and Warhurst, D.C. *Ann. Trop. Med. Hyg.* 1986, **80,** 483
15 Fitch, C.D. *Parasitol. Today* 1986, **2,** 330
16 Warhurst, D.C. *Biochem. Pharmacol.* 1981, **30,** 3323
17 Zhang, F., Gosser, D.K., Jr., and Meshnick, S.R. *Biochem. Pharmacol.* 1992, **43,** 1805
18 Chemical Design, Inc., Mahwah, NJ, USA
19 Tripos Associates, St. Louis, MO, USA
20 Cambridge Crystallographic Data Centre, University Chemical Laboratory, Lansfield Rd., Cambridge CB2, England
21 Fersht, A.R. *Trends Biochem. Sci.* 1984, **9,** 145
22 Fersht, A.R., Shi, J., Knill-Jones, J., Lowe, D.M., Wilkinson, A.J., Blow, D.M., Brick, P., Carter, P., Wayne, M.M.Y., and Winter, G. *Nature (London)* 1985, **314,** 235
23 Street, I.P., Armstrong, C.R., and Withers, S.G. *Biochemistry* 1986, **25,** 6021
24 Scheer, H. and Katz, J.J. In *Porphyrins and Metalloporphyrins* (K. Smith, Ed.), Elsevier Scientific, Amsterdam, 1975, p 399
25 Slater, A.F.G., Swiggard, W.J., Orton, B.R., Flitters, W.D., Goldberg, D.E., Cerami, A., and Henderson, G.B. *Proc. Natl. Acad. Sci. U.S.A.* 1991, **88,** 325